JOURNAL OF APPLIED ELECTROCHEMISTRY **28** (1998) 935–941

Effects of incorporation of Cu and Ag in Pd on electrochemical oxidation of methanol in alkaline solution

J. PRABHURAM, R. MANOHARAN*

HEB R&D Laboratories, High Energy Batteries (I) Ltd, Mathur 622 515, Pudukkottai Dt., Tamil Nadu, India

H. N. VASAN

Solid State and Structural Chemistry Unit, Indian Institute of Science, Bangalore 560 012, India

Received 30 May 1997; revised 16 December 1997

Pd fine particles were prepared by heterogeneous reaction of PdO_x with dry methanol as well as by the $NaBH_4$ reduction method. The former method was found to give Pd nanoparticles (~5 nm). Similarly f.c.c. structured, single phase nanoparticles of alloy compositions $Pd_{0.8}Cu_{0.2}$, $Pd_{0.5}Cu_{0.5}$, $Pd_{0.8}Ag_{0.2}$ and $Pd_{0.5}Ag_{0.5}$ were prepared by the heterogeneous reaction of dry methanol with intimate mixtures of $PdO_x + CuO_x$ and $PdO_x + AgNO_3$. The electrochemical properties of the porous unsupported electrodes, prepared from these materials, in alkaline solutions, were investigated by cyclic voltammetry and steady-state polarization measurements. Various processes taking place during potential scanning in the presence and absence of methanol in 6 M KOH solution are discussed. Steady-state polarization data indicate that the methanol oxidation reaction (MOR) activity decreases with incorporation of Cu and Ag into the Pd lattice. The extent of decrease in the MOR activity is less for Cu addition than for Ag addition.

Keywords: *Pd electrodes*, *Cu and Ag incorporation*, *methanol oxidation*, *alkaline electrolyte*, *cyclic voltammetry*, *steady-state polarization*

1. Introduction

Although Pd is a suitable electrocatalyst for oxidising small organic molecules [1–9], cyclic voltammetric (CV) properties of unsupported porous Pd electrodes and its binary alloy electrodes have been far less intensively investigated than Pt and its alloy electrodes for electrocatalysis of methanol oxidation reaction (MOR). In the present study, Pd + Cu and Pd + Ag nanoparticle alloys were prepared in single phases possessing f.c.c. structure by the heterogeneous reaction of $AgNO_3 + PdO_x$ or $CuO_x + PdO_x$ mixtures with dry methanol or ethanol under refluxing conditions at ambient temperature [10]. The unsupported electrodes were then prepared without dispersing the catalysts Pd, $Pd_{0.8}Cu_{0.2}$, $Pd_{0.5}Cu_{0.5}$, $Pd_{0.8}Ag_{0.2}$ and $Pd_{0.5}Ag_{0.5}$ on carbon substrates and changes in the MOR activities and in single cyclic votammetric characteristics in 6 M KOH/1 M CH_3OH were examined.

2. Experimental details

Pd powder was prepared by two methods: (i) by reducing 1% $PdCl_2$ solution with 5% $NaBH_4$ solution and thoroughly washing the precipitate with pure water, and (ii) by refluxing PdO_x in dry methanol at room temperature for 10 h. The PdO_x required for this purpose was prepared by concentrating an aqueous solution of $Pd(NO_3)_2$ followed by decomposition around 333 K.

Powders of Pd + Cu alloys of compositions $Pd_{0.8}Cu_{0.2}$ and $Pd_{0.5}Cu_{0.5}$ and Pd + Ag alloys of compositions $Pd_{0.8}Ag_{0.2}$ and $Pd_{0.5}Ag_{0.5}$ were prepared by the procedure reported elsewhere [10]. In a typical preparation of Pd + Ag particles, 30 ml of an aqueous solution of $Pd(NO_3)_2$ (1.13 m mol in Pd) was mixed with the stoichiometric quantity of $AgNO_3$ (as required for $Pd_{0.8}Ag_{0.2}$ and $Pd_{0.5}Ag_{0.5}$ compositions) and the solution made up to 50 ml. The solution containing the two nitrates was slowly concentrated under stirring and dried around 333 K. At this temperature, the Pd nitrate decomposed to PdO_x, giving a mixture of $AgNO_3$ and PdO_x. This mixture was stirred for 12 h in 200 ml of dry methanol and then refluxed for 180–200 h. At the end of the reaction, the homogeneous particles settled down. The particles were washed with dry methanol and stored in methanol.

In the preparation of $Pd_{0.8}Cu_{0.2}$ and $Pd_{0.5}Cu_{0.5}$ alloy particles, a solution of Cu nitrate (prepared by dissolving the stoichiometric quantity of Cu powder

* To whom correspondence should be addressed.

0021-891X

in HNO_3) was added to the Pd nitrate solution. The solution of the two nitrates when concentrated and dried and gave an intimate mixture of CuO_x and PdO_x. This oxide mixture was refluxed with dry ethanol under dry nitrogen.

The single phase alloys were confirmed by running X-ray diffraction patterns and comparing with the patterns reported earlier [10].

The catalytic particles were also characterized by TEM and EDX analysis to obtain particle size and composition information. Electron micrographs of the catalytic particles indicated that all the materials, except the Pd particles prepared by $NaBH_4$ reduction, were nanoparticles. The particle size of the Pd powders prepared by the reaction of PdO_x with methanol was ~5 nm. The particle sizes of Pd + Ag of different compositions were generally in the range 10–40 nm and those of the Pd + Cu particles were in the range 5–15 nm.

The EDX analysis of surface compositions of alloy particles showed that the Ag : Pd or Cu : Pd ratios were very close to those in the starting compositions, indicating completeness of the reaction and also the absence of surface enrichment.

The unsupported electrodes of Pd, Pd + Cu and Pd + Ag alloys were prepared by directly pressing the powders over Pt expanded metal grids (0.05 mm diameter wire, 400 mesh cm^{-2}) at 450 psi at room temperature for 5 min. The porosity of these electrodes was found to be 50% (estimated by taking the ratio of measured density and the density corresponding to the actual materials taken for making the electrodes). The real area of the electrodes was not determined in the present study and the geometrical area was utilised to calculate the current densities.

Porous Ag electrodes (thickness 0.52 mm) were prepared by the roll mill technique. Ag powder was first spread on Ag expanded metal grid (0.52 mm diameter, 16 mesh cm^{-2}), compacted in the roll mill and sintered at 800 °C. Copper electrodes were prepared from a pure copper foil (thickness 0.2 mm, purity 99.9%)

A conventional three electrode electrochemical cell with a $Hg/HgO/OH^-$ reference electrode, and a sintered Ni sheet of high surface area as counter electrode were employed to evaluate the performances of electrodes in 6 M KOH. 1 M CH_3OH was mixed with the electrolyte when required and nitrogen gas was purged for 2 h prior to the measurements. This electrolyte/methanol mixture was chosen as the unsupported Pd electrodes yielded better performances in this mixture than similarly prepared unsupported Pt electrodes. The effect of variation of reactant concentration and sweep rate is discussed elsewhere [11]. Cyclic voltammograms (CVs) were recorded with a BAS model 100 B/W potentiostat interfaced to an IBM PxT microcomputer with a National Instruments IEEE-488 General-purpose Interface (GPIB) card. The BAS Electrochemistry Software was used to drive the measurements, process the data and display the CV curves.

3. Results and discussion

3.1. *Electrocatalysis in 6 M KOH solution in the absence of methanol*

Figure 1 shows the fifth CV cycles for the unsupported Pd electrodes. Pd prepared by both $NaBH_4$ and dry methanol reduction methods gave identical features. The features during the forward sweep are observed to be present in similar potential regions for both Pd electrodes. An oxidation current commences at −0.76 V and then slowly rises, leading to a peak with E_p about −0.4 V and a shoulder with E_p about −0.34 V. The current then decreases until E = −0.25 V is reached. At E > −0.25 V, a current plateau is formed. During the backward scan, for Pd prepared by $NaBH_4$ reduction, a broad reduction peak with E_p = −0.26 V is observed which is followed by a double layer region and another reduction peak with E_p = −0.79 V. For Pd prepared by the dry methanol reduction method, both reduction peaks are shifted positively by about 70 mV.

Initially, in the region of commencement of the oxidation current, oxidation of absorbed hydrogen takes place. This is then followed by formation of premonolayer surface hydroxide species (active oxide species) in the areas of peaks with E_p = −0.4 and −0.34 V. According to Burke *et al.* [3, 12], the associated electrochemical processes occurring in these regions are

$$Pd + OH^- \leftrightarrow PdOH + e^- \quad (1)$$

$$Pd^* + 6\,OH^- \leftrightarrow [Pd(OH)_6]^{2-} + 4\,e^- \quad (2)$$

It has been argued that Reaction 2 takes place as a result of an adatom/incipient hydrous oxide transition which is dependant largely on the metal atom displacement effect arising from the repetitive formation and reduction of thin compact layers [3]. This reaction occurs as the metal atoms at the interface

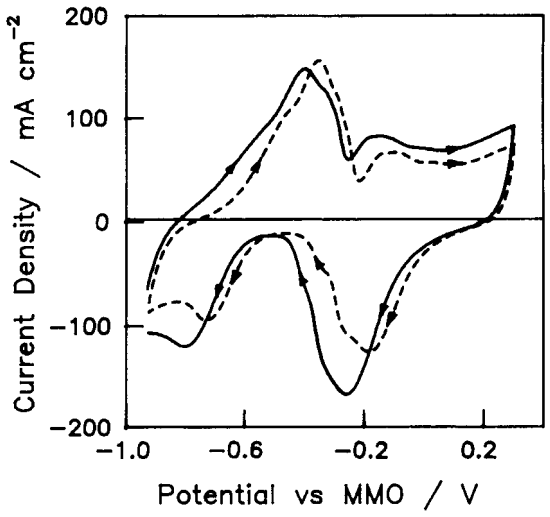

Fig. 1. 5th cycle CVs for the unsupported Pd electrodes in 6 M KOH solution at room temperature in the range −0.926 to 0.304 V, scan rate 25 mV s^{-1}. (——) Pd prepared by $NaBH_4$ reduction method and (- - -) Pd prepared by dry methanol reduction method.

decrease their lattice coordination numbers and attain the adatom state. The population of these types of surface active atoms is significantly less on bright palladium electrodes and large in the case of palladized palladium electrodes, due to the possibility of surface defect formation. In the present study, Pd powder was prepared at low temperature and, therefore, the chances of more surface defects are high.

In the plateau region, that is, at $E > -0.25$ V, monolayer oxide deposition takes place [12–16]. During the backward sweep, this oxide layer is reduced in the region 0.2 to −0.48 V for Pd prepared by the $NaBH_4$ method, and in the region 0.2 to −0.4 V for Pd prepared by the dry methanol reduction method. In the lower potential region, where the other reduction peak is observed, Reaction 2 is shifted to the left and the hydroxide species $[Pd(OH)_6]^{2-}$ that are attached to the metal lattice are reduced and Pd adatoms (Pd^*) are formed on the Pd surface [3, 17]. The reduction of $[Pd(OH)_6]^{2-}$ species takes place at relatively positive potentials on the nanoparticle Pd prepared by the methanol reduction method which is likely to possess more surface defects. Finally, after a few cycles, hydrogen absorption [3, 16, 18] takes place at a low level at $E < -0.87$ V for Pd prepared by the $NaBH_4$ method and at $E < -0.83$ V for nanoparticle Pd prepared by the dry methanol reduction method.

It is of interest to look at the first CV cycles in Fig. 2 recorded for the Pd electrodes. In the first cycle, as soon as the forward scan is started from $E = -0.926$ V, hydrogen absorption takes place vigorously on Pd prepared by $NaBH_4$ method. The absorption rate begins to decrease at $E = -0.83$ V and reaches zero as the potential scan reaches $E = -0.71$ V, beyond which desorption of hydrogen begins. At the end of the first cycling, the hydrogen absorption rate is drastically reduced when the potential becomes negative. It seems that the entry of hydrogen into the palladium is partially blocked after the first cycle due to the fact that some of the active oxide deposit is not completely reduced at the lower end of the negative sweep. In the 2nd cycle, the rate decreases further and after the 3rd cycle stable current values are established. Similar hydrogen absorption–desorption behaviour is observed on Pd prepared by the dry methanol reduction method also.

In the case of Cu, Cu_2O and a mixture of CuO and $Cu(OH)_2$ form [19–23] in the region −0.44 to −0.3 V and −0.22 to 0.2 V, respectively, during the forward scan. In the backward scan, surface corrosion reaction is reactivated in the region 0.14 to −0.18 V and reduction reaction of Cu–oxygen species to Cu metal occurs in between −0.65 and −0.75 V [23–25].

When Pd and Cu elements are alloyed, CVs having totally different features are observed. For example, the CV of the alloy $Pd_{0.8}Cu_{0.2}$ in Fig. 3 does not exhibit peaks corresponding to the reactions on individual elements Pd and Cu; it exhibits a broad anodic peak in the region −0.83 to −0.35 V where active oxygen atoms coverage takes place on all the Pd sites and another anodic feature which slowly raises from −0.3 V that can be speculated to be due to the formation of a thick Pd + Cu mixed oxide layer on the alloy surface. Upon reversing the scan, reduction of this oxide takes place and a fairly broad peak with $E_p = -0.5$ V was observed.

On lowering the Pd concentration in the alloy, as in $Pd_{0.5}Cu_{0.5}$, the active oxygen atoms coverage is lowered in the region −0.83 to −0.35 V.

From Fig. 4, it is clear that silver electrodes do not take oxygen atoms from the water in the MOR potential region between −0.926 and 0.3 V and therefore incorporation of Ag into the Pd lattice will exert a negative influence. Replacing Pd atoms by Ag atoms will only reduce the population of active Pd sites on which active oxygen atoms can sit and this is evident in the CVs for $Pd_{0.8}Ag_{0.2}$ and $Pd_{0.5}Ag_{0.5}$ in Fig. 5(a)

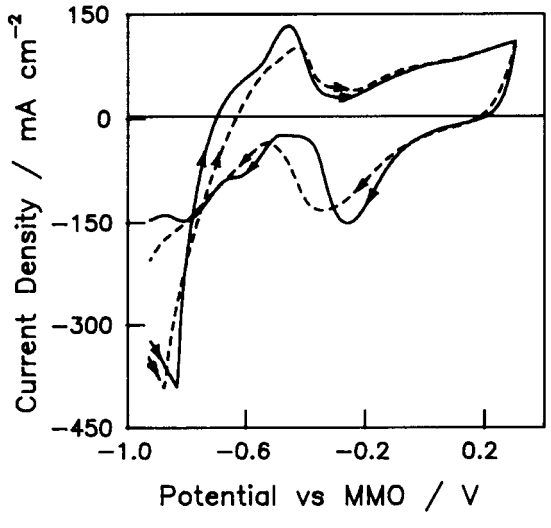

Fig. 2. 1st cycle CVs for the unsupported Pd electrodes in 6 M KOH solution at room temperature in the range −0.926 to 0.304 V, scan rate 25 mV s^{-1}. (——) Pd prepared by $NaBH_4$ reduction method and (- - - -) Pd prepared by dry methanol reduction method.

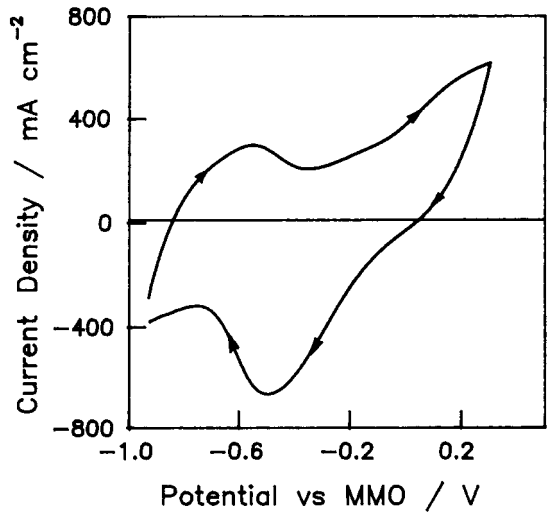

Fig. 3. CV for an unsupported $Pd_{0.8}Cu_{0.2}$ electrode in 6 M KOH solution at room temperature in the range −0.926 to 0.304 V, scan rate 25 mV s^{-1}. (5th cycle).

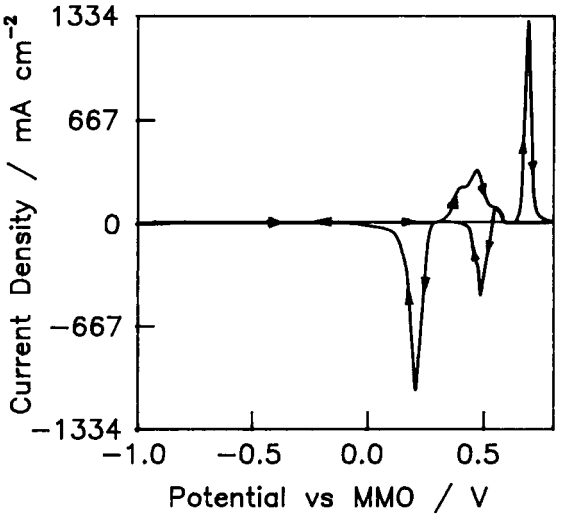

Fig. 4. CV for a porous Ag electrode in 6 M KOH solution at room temperature in the range −0.926 to 0.8 V, scan rate 25 mV s^{-1}. (5th cycle).

and (b). For the Pd + Ag alloys also, as in the case of Pd + Cu alloys, the Pd character in the CV decreases as the Ag composition is increased.

On Pd + Cu and Pd + Ag alloys also, the hydrogen absorption reaction takes place in the negative potential region in the first cycle and it is suppressed during the further cycling.

3.2. *Electrooxidation of methanol in 6 M* KOH + *1 M* CH_3OH *solution*

The CV obtained for the MOR on a Pd electrode (Pd prepared by the $NaBH_4$ reduction method) is shown in Fig. 6. During the forward sweep, initially an anodic peak,O_1^f, the onset potential and E_p of which are −0.7 and 0 V, respectively. The presence of active oxide species on palladium at low potentials greatly helps to oxidise methanol effectively. Methanol molecules chemisorptively dissociate on the Pd sites by interacting with the surface OH species as follows [4]:

$$2\,Pd + CH_3OH \rightarrow Pd\text{–}(CH_3O)_{ads} + PdH \quad (3)$$

$$Pd\text{–}(CH_3O)_{ads} + PdOH \rightarrow Pd_2\text{–}(CH_2O)_{ads} + H_2O \quad (4)$$

$$Pd_2\text{–}(CH_2O)_{ads} + PdOH \rightarrow Pd_3\text{–}(CHO)_{ads} + H_2O \quad (5)$$

$$Pd_3\text{–}(CHO)_{ads} + PdOH \rightarrow Pd_2(CO)_{ads} + 2\,Pd + H_2O \quad (6)$$

$$Pd_2(CO)_{ads} + PdOH \rightarrow PdCOOH + 2\,Pd \quad (7)$$

$$PdCOOH + OH^- \rightarrow Pd + CO_2\uparrow + H_2O + e^- \quad (8)$$

An *in situ* IR spectroscopic study by Enyo *et al.* [4] on a bright Pd electrode has revealed out that the CO species are bridge bonded to Pd sites and not linearly bonded. These bridge bonded Pd_2CO species act as poisonous species.

Reactions 3 to 6 appear to occur in the potential region of the peak O_1^f in Fig. 6. Steps 7 and 8 also take place to some extent in this potential region.

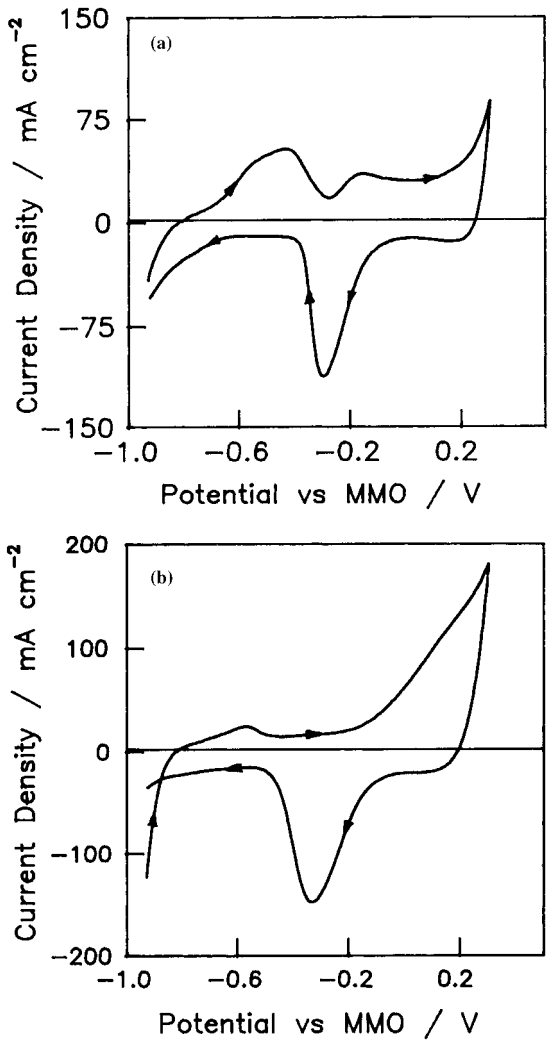

Fig. 5. CVs for the unsupported (a) $Pd_{0.8}Ag_{0.2}$ electrode and (b) $Pd_{0.5}Ag_{0.5}$ electrode in 6 M KOH solution at room temperature in the potential range −0.926 to 0.304 V, scan rate 25 mV s^{-1}. (5th cycles).

Complete removal of CO species may not be possible here as they strongly bind the electrode surface.

At $E > 0.025$ V, the formation of the active oxide mediator is severely impeded due to the onset of formation of the regular monolayer oxide film and hence anodic current drops sharply. However, highly active oxygen atoms again become available at $E > 0.4$ V (just before the occurrence of oxygen evolution reaction), and the poisonous bridge bonded Pd_2CO species are oxidized by the reaction

$$Pd_2CO + 3OH^- \rightarrow PdOH + Pd + CO_2\uparrow + H_2O + 3\,e^- \quad (9)$$

as is evident from the appearance of another anodic peak, O_2^f in the CV of Fig. 6.

During the backward sweep, the monolayer oxide film is reduced and the corresponding cathodic current is compensated by the anodic current of Reaction 9 which may also take place simultaneously utilising the least OH^- ions available on the monolayer oxide film. As the potential scan reaches about −0.35 V, all the inactive oxide film will be reduced and plenty of the active oxygen atoms become

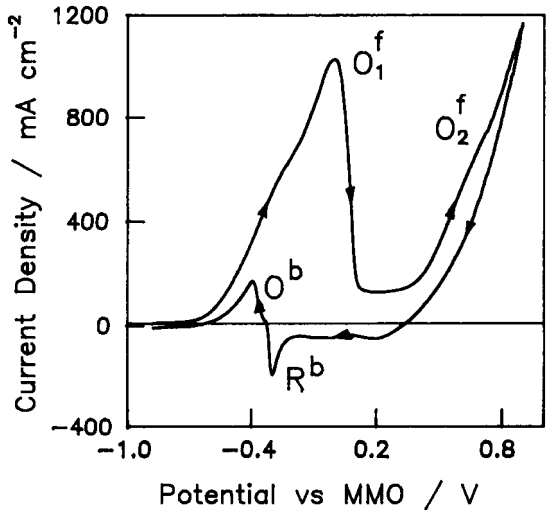

Fig. 6. CV for the MOR on an unsupported Pd in 6 M KOH + 1 M CH_3OH solution at room temperature in the range −0.886 to 0.9 V, scan rate 25 mV s^{-1}. (5th cycle).

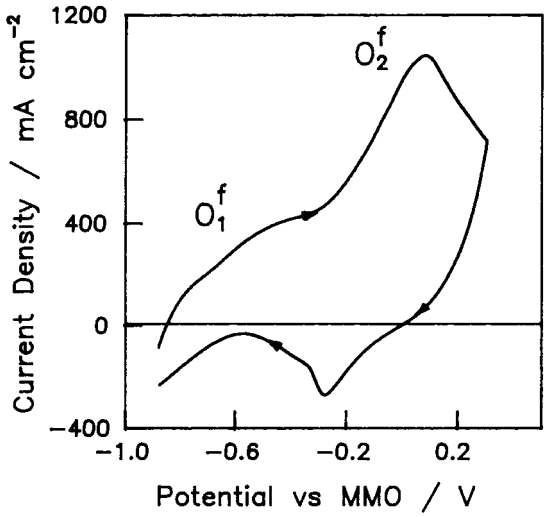

Fig. 7. CV for the MOR on an unsupported $Pd_{0.8}Cu_{0.2}$ electrode electrode in 6 M KOH + 1 M CH_3OH solution at room temperature in the range −0.886 to 0.304 V, scan rate 25 mV s^{-1}. (5th cycle).

available at Pd free sites causing Reaction 9 to resurgent; this gives rise to an oxidation O^b peak.

The cathodic peak, R^b, with $E_p = -0.3$ V of Fig. 6 is due to reduction of reducible organic species which might have formed in the higher potential region [26].

A shoulder occurs somewhere in the region about −0.6 to −0.15 V in this CV and this may be attributed to the oxidation arising out of the condition when OH^- ions are available in excess and chemisorbed organic species are available insufficiently at the electrode surface in the taken electrolyte solution [11].

A comparison of CVs recorded for the MOR on Pd electrodes prepared from powders synthesized via both preparative methods exhibited identical features. However, electrodes prepared from Pd nanoparticles yield higher magnitude of oxidation current suggesting that the electrodes consisting of Pd nanoparticles can yield higher MOR activity.

The features of CV in Fig. 7 for the MOR on a $Pd_{0.8}Cu_{0.2}$ alloy electrode are entirely different. During the forward sweep, two broad oxidation peaks O_1^f and O_2^f are observed in the range −0.926 to 0.304 V. It appears that the peak O_1^f is associated with Steps 3–6 of the MOR mechanistic pathways. The peak O_2^f that lies in the region −0.25 to 0.3 V with $E_p = 0.07$ V may be associated with Steps 7 and 8 of the MOR pathways. The anodic current, in contrast to the Pd electrodes, does not fall down sharply for $Pd_{0.8}Cu_{0.2}$ after the appearance of E_p and the current is observed until 0.3 V. Also, no oxidation current is observed for $Pd_{0.8}Cu_{0.2}$ during the backward sweep. Instead, two reduction peaks, one with $E_p = -0.3$ V and another reduction profile at potentials negative of −0.55 V, are formed and they may be due to the occurrence of reduction of reducible organic carbon residues which are facilitated by the surface Cu species [27].

When Ag is bonded to Pd as in $Pd_{0.8}Ag_{0.2}$ and $Pd_{0.5}Ag_{0.5}$, Ag atoms block both the methanol absorbing and the active oxygen extracting sites and therefore lesser currents are observed for the MOR in the CVs of these alloy electrodes. A couple of changes in the features of the CVs of Ag doped alloy electrodes are noticed during the occurrence of the MOR. The shoulder which is seen in Fig. 6 is missing in the CVs of Pd + Ag alloys, see for instance the CV in Fig. 8. Also, as in the case of Pd + Cu alloy electrodes, the current does not fall down sharply after the appearance of E_p of the O^f peak in the CV of the Pd + Ag alloy electrodes and this may be attributed to the inability to form monolayer oxide film.

Steady-state galvanostatic polarisation curves for the electrooxidation of methanol at room temperature in 6 M KOH + 1 M CH_3OH are compared in Fig. 9 for Pd, Pd + Cu and Pd + Ag alloy electrodes. Also shown in this Figure is a polarization curve for a Pd electrode prepared from the powder synthesised by $NaBH_4$ reduction method.

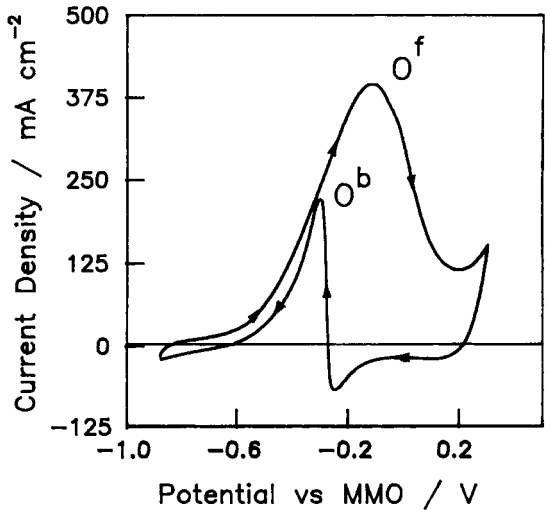

Fig. 8. CV for the MOR on an unsupported $Pd_{0.8}$ $Ag_{0.2}$ electrode in 6 M KOH + 1 M CH_3OH solution at room temperature in the range −0.886 to 0.304 V, scan rate 25 mV s^{-1}. (5th cycle).

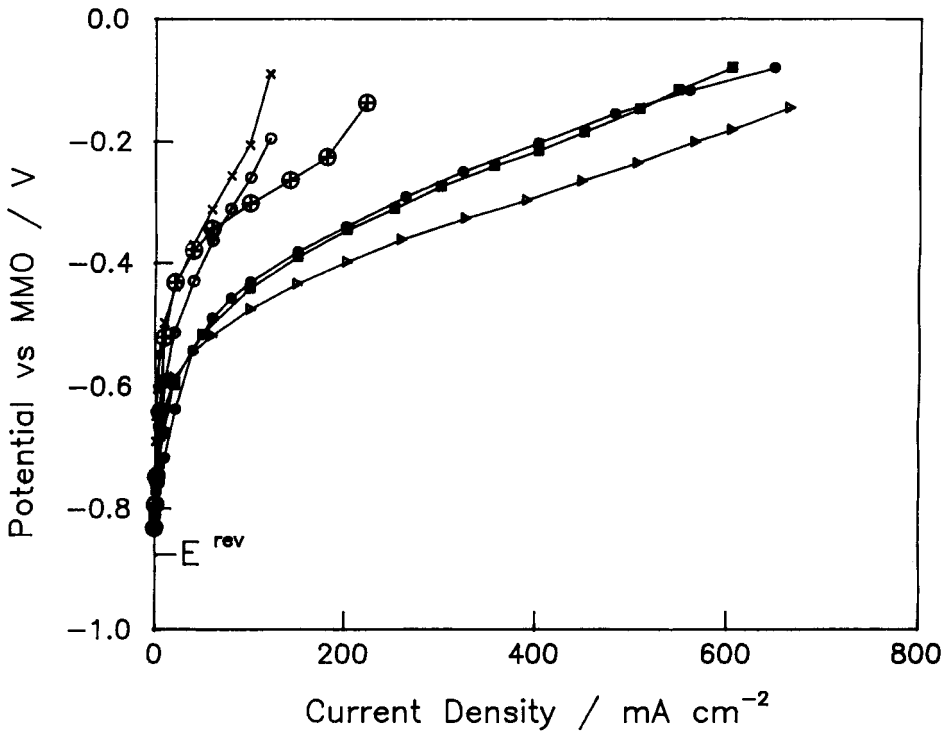

Fig. 9. The MOR polarization curves for the unsupported nanoparticle Pd, Pd + Cu and Pd + Ag alloy electrodes and for a Pd electrode made out of powder prepared by $NaBH_4$ reduction method in 6 M KOH + 1 M CH_3OH. Key: (■–■) Pd ($NaBH_4$ reduction); (▶–▶) Pd (CH_3OH reduction); (●–●) $Pd_{0.8}Cu_{0.2}$; (⊕–⊕) $Pd_{0.5}Cu_{0.5}$; (○–○) $Pd_{0.8}Ag_{0.2}$; (×–×) $Pd_{0.5}$ $Ag_{0.5}$. All at 30 °C.

Figure 10 shows the variation of the MOR current density at the overpotential $\eta = 0.7$ V, taken from steady-state data, with Pd content in Pd + Cu and Pd + Ag alloy electrodes. The MOR activity decreases with the incorporation of Ag and Cu in the lattice of palladium. In terms of the MOR electrocatalysis, Cu seems to be a better additive than Ag for the following reasons. In the case of Ag incorporation, the MOR activity decreases quite drastically as Ag does not participate in any form in the MOR mechanistic pathways in the potential region of interest. Whereas, in the case of Cu addition, the extent of decrease in the MOR activity is less suggesting that in addition to some Pd sites in Pd + Cu alloys, Cu atoms present in the anodically formed surface Pd + Cu mixed oxide film also helps to extract oxygen atoms from the electrolyte and supply the same to the adjacent Pd sites for burning off of the carbonaceous organic residual species.

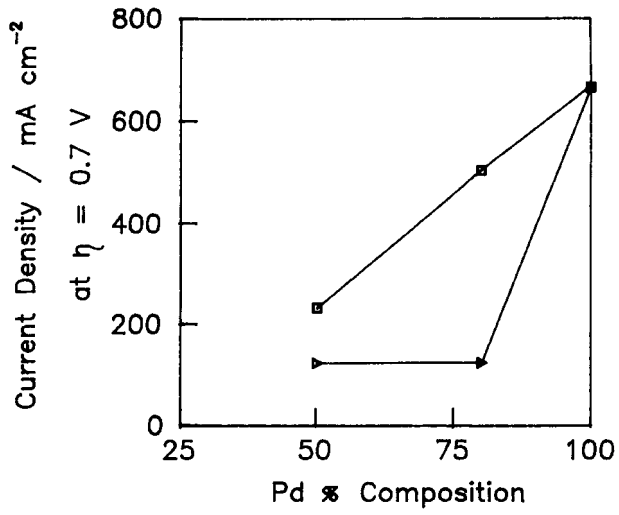

Fig. 10. Variation of the MOR activity (expressed in terms of anodic current density at $\eta = 0.7$ V) with the Pd content in Pd + Cu and Pd + Ag alloy electrodes in 6 M KOH + 1 M CH_3OH solution. Key: (□–□) Pd–Cu; (▷–▷) Pd–Ag.

4. Conclusions

The present study has demonstrated the following facts:

(i) The novel low temperature preparative methods adopted for preparing Pd + Ag and Pd + Cu alloy particles in this study have enabled us to carry out detailed electrochemical measurements on single phase materials to assess their cyclic voltammetric and the MOR electrocatalytic properties.

(ii) The nanoparticle Pd shows a superior performance for the MOR in 6 M KOH solution than the Pd prepared by the $NaBH_4$ reduction method.

(iii) On alloying Pd with Cu, marked differences have been observed in the CVs of alloys in 6 M KOH solution. Pd + Cu mixed layer formation is observed during the forward sweep which is preceded by the active oxygen coverage on Pd sites in the low potential region. On lowering the Pd concentration in the alloy, Pd character in the CV is reduced. In the case of Pd + Ag alloys also, the Pd character in the CV decreases as the Ag composition is increased.

(iv) The MOR activity decreases on alloying Pd with Ag or Cu. The activity decreases drastically on Ag addition and the extent of activity reduction is less for Cu addition.

References

[1] K. Nishimura, K. Machida and M. Enyo, *J. Electroanal. Chem.* **251** (1988) 103.
[2] F. Kadirgan, B. Beden, J. M. Leger and C. Lamy, *ibid.* **125** (1981) 89.
[3] L. D. Burke and K. J. O' Dwyer, *Electrochim. Acta* **35** (1990) 1821.
[4] K. Nishimura, K. Kunimatsu and M. Enyo, *J. Electroanal. Chem.* **260** (1989) 167.
[5] M. I. Manzanares, A. G. Pavese and V. M. Solis, *ibid.* **310** (1991) 159.
[6] M. Enyo, *ibid.* **186** (1985) 155.
[7] T. Takamura and Y. Sato, *Electrochim. Acta* **19** (1974) 63.
[8] T. Takamura and K. Minamiyama, *J. Electrochem. Soc.* **112** (1965) 333.
[9] T. Takamura and F. Mochimaru, *ibid.* **114** (1967) 1251.
[10] H. N. Vasan and C. N. R. Rao, *J. Mater. Chem.* **5**(10) (1995) 1755.
[11] J. Prabhuram and R. Manoharan, *J. Power Sources* (in press).
[12] L. D. Burke and J. K. Casey, *J. Appl. Electrochem.* **23** (1993) 573.
[13] R. Woods in 'Electroanalytical Chemistry' (edited by A. J. Bard), Marcel Dekker, New York, **9** (1976) chapter 1.
[14] G. Belanger and A. K. Vijh, *in* 'Oxide and Oxide Films' (edited by A. K. Vijh), Marcel Deckker, New York, **5** (1977) chapter 1.
[15] L. D. Burke, in 'Electrodes of Conductive Metalic Oxides, Part A' (edited by S. Trasatti), Elsevier, Amsterdam (1980) chapter 3.
[16] L. D. Burke and J. K. Casey, *J. Electrochem. Soc.* **140** (1993) 1292.
[17] L. D. Burke and M. B. C. Roche, *J. Electroanal. Chem.* **186** (1985) 139.
[18] V. Chausse, P. Regull and L. Victori, *J. Electroanal. Chem.* **238** (1987) 115.
[19] B. Miller, *J. Electrochem. Soc.* **116** (1969) 1675.
[20] N. A. Hampson, J. B. Lee and K.I. MacDonald, *J. Electroanal. Chem.* **32** (1971) 165.
[21] J. Ambrose, R. G. Barradas and D. W. Shoesmith, *ibid.* **47** (1973) 47.
[22] L. D. Burke, M. J. G. Ahern and T. G. Ryan, *J. Electrochem. Soc.* **137** (1990) 553.
[23] L. D. Burke and T. G. Ryan, *ibid.* **137** (1990) 1358.
[24] D. D. MacDonald, *ibid.* **121** (1974) 651.
[25] A. M. Castro Luna de Medina, S. L. Marchiano and A. J. Arvia, *J. Appl. Electrochem.* **8** (1978) 121.
[26] K. Ohkawa, K. Hashimoto, A. Fujishima, Y. Nogunchi and S. Nakayama, *J. Electroanal. Chem.* **345** (1993) 445.
[27] K. W. Frese and Jr, *J. Electrochem. Soc.* **138** (1991) 3338.